Available online at www.sciencedirect.com
ScienceDirect
Journal of Molecular Catalysis A: Chemical 282 (2008) 67–73
JOURNAL OF MOLECULAR CATALYSIS A: CHEMICAL
www.elsevier.com/locate/molcata

Stability of Pt particles on ZrO_2 support during partial oxidation of methane: DRIFT studies of adsorbed CO

Xinli Zhu [a], Yongbing Xie [a], Chang-jun Liu [a,*], Yue-ping Zhang [b]

[a] *Key Laboratory for Green Chemical Technology of Ministry of Education, School of Chemical Engineering, Tianjin University, Tianjin 300072, China*
[b] *Department of Chemistry, Tianjin University, Tianjin 30072, China*

Received 13 March 2007; received in revised form 18 November 2007; accepted 23 November 2007
Available online 10 January 2008

Abstract

In this work, diffuse reflectance infrared Fourier transformation (DRIFT) spectroscopy of adsorbed CO was studied to investigate the stability of Pt/ZrO_2 catalysts for partial oxidation of methane. The studies confirmed that the preparation method has a significant effect on the catalyst performance and the catalyst treatment using argon glow discharge plasma improves the catalyst stability. TG analysis showed that coke formation is not significant on both samples with and without glow discharge plasma treatment, indicating the coke formation is not responsible for the catalyst deactivation. The IR band intensity of adsorbed CO decreases remarkably with increasing calcination temperature, suggesting the sintering of Pt particles in the presence of O_2. The sintering of plasma treated sample is slower than that of the untreated sample, especially at higher temperature, which indicates that the plasma treated sample is more resistant to sintering under the oxidizing atmosphere.

Keywords: Partial oxidation; Methane; Pt/ZrO_2; Plasma treatment; Glow discharge; Deactivation; DRIFT; Synthesis gas; Sintering

1. Introduction

Synthesis gas (CO and H_2) is now industrially produced through steam reforming of methane, which has some obvious drawbacks, such as intense energy input and high H_2/CO ratio for further synthesis [1]. Catalytic partial oxidation of methane (POM) to synthesis gas (1) is a promising alternative to steam reforming. The weak exothermic property of POM leads to some advantages, such as lower energy input and higher operating space velocity [2,3]. In addition, the theoretical H_2/CO ratio of this reaction is 2, which is very suitable for further synthesis of hydrocarbons and/or oxygenated hydrocarbons.

$$CH_4 + \tfrac{1}{2}O_2 \rightarrow CO + 2H_2 \quad (\Delta H^{\circ}_{298\,K} = -35\,\text{kJ mol}) \qquad (1)$$

Pt/ZrO_2 is an active and stable catalyst for CO_2 reforming of methane [4–6]. It has been tested for POM. However, a quick deactivation was usually observed [7–9]. A two-step reaction mechanism was proposed for POM over Pt/ZrO_2; CH_4 is directly oxidized to CO_2 and H_2O in the first step, and then CO_2 reforming and steam reforming of the left CH_4 occurs in the second step [9,10]. Both CO_2 and steam reforming of CH_4 are highly endothermic reactions, and thus the potential of coke formation is high at high reaction temperature. Coke formation has been suggested as the deactivation reason for POM over Pt/ZrO_2 [9]. However, little attention has been paid to the Pt sintering in the presence of O_2 for POM over Pt/ZrO_2.

Because of the high price and low availability, reduction in the amount of Pt usage is highly desirable. However, characterization of supported catalysts with a small amount of metal is very difficult since the small amount limits characterization methods, such as X-ray powder diffraction (XRD). Infrared (IR) spectroscopy using CO as probe molecule is a well established method for characterizing supported metal catalysts [11–15]. The IR spectrum of adsorbed CO is very sensitive to the particle size, morphology, and electronic structure, and this information can be obtained in turn.

On the other hand, preparation methods show a significant influence on the performance of catalysts for partial oxidation of methane [16]. We previously observed a remarkable improvement in the activity and stability of catalysts for POM can be achieved by using glow discharge plasma treatment of the catalyst [17,18]. Glow discharge is one of non-thermal

* Corresponding author. Fax: +86 22 27890078.
E-mail addresses: coronacj@tju.edu.cn, ughg_cjl@yahoo.com (C.-j. Liu).

1381-1169/$ – see front matter © 2007 Elsevier B.V. All rights reserved.
doi:10.1016/j.molcata.2007.11.020

plasma phenomena, characterized by high electron temperature (10,000–100,000 K) and low gas temperature (as low as room temperature) [19]. Catalyst preparation using non-thermal plasma treatment attracts increasing attentions in recent years [17–24]. The energetic species (electrons, ions, and radicals) in plasmas could modify the metal particle size, morphology, and metal-support interactions of catalysts [20], leading to some specific catalytic properties.

The aim of this work is to study the structure and stability of the Pt/ZrO_2 catalyst for POM using IR spectra of adsorbed CO. The enhanced stability of Pt/ZrO_2 catalysts via glow discharge plasma treatment has also been investigated.

2. Experimental

2.1. Catalyst preparation

ZrO_2 (S_{BET} = 8.3 m^2/g, monoclinic) was purchased from Alfa Aesar, and used as received. It was impregnated at room temperature for 12 h with aqueous solution of $H_2PtCl_4{\bullet}6H_2O$ (99%, Tianjin North China Reagent Co.), followed by drying at 110 °C for another 12 h. The resulting sample was divided into two parts. One part was directly calcined in a muffle at 600 °C for 4 h (denoted by PtZr-C), while the other part was treated with argon glow discharge plasma for 1 h followed by calcination at 600 °C for another 4 h (denoted by PtZr-PC). The amount of Pt loading is 0.5 wt%. Sometimes the calcination was carried out at 400 °C for 4 h or at 800 °C for 4 h after calcination at 600 °C for 4 h, which was specially addressed in the text.

The plasma treatment was carried out in a glow discharge system as described previously [17]. Briefly, 1 g catalyst sample loaded in a quartz boat was put in the discharge cell. When the pressure was adjusted in the range of 200–100 Pa, glow discharge plasma was ignited by applying voltage of 900 V to the electrodes. The 100 Hz square wave signal was generated by a function/arbitrary waveform generator (Hewlett Packard, 33120A), and amplified to 900 V by a high voltage amplifier (Trek, 20/20B). High purity argon was used as plasma forming gas. Each treatment lasted 10 min, and the treatment was repeated 6 times.

2.2. Activity test

The activity test was carried out in a micro tubular quartz reactor (inner diameter is 4 mm) at atmospheric pressure. The catalyst sample of 40 mg (40–60 mesh) was packed in the reactor with two layers of quartz wool. Prior to reaction, the catalyst was reduced by using flowing H_2 (30 cm^3/min) at 500 °C for 1 h. Then the temperature was increased to 800 °C under flowing argon. When the temperature was stabilized, CH_4 and O_2 with a ratio of 2:1 were introduced to the micro reactor by mass flow controllers. The gases after reaction passed through an ice trap to remove water, and was then analyzed at every 30 min by a gas chromatograph (Angilent 6890N), equipped with a thermal conductivity detector and a 2-m TDX-01 packed column. When the reaction was stopped, the temperature was slowly decreased to room temperature under protection of flowing argon. All gases used are in ultrahigh purity, without further purification.

2.3. Characterizations

The dispersion of Pt was measured using a volumetric system (Quantachrome, Autosorb-1). The catalyst sample was firstly reduced at 300 °C for 2 h. Then the CO chemisorption was performed at 40 °C. The ratio of CO:Pt = 1:1 was used to calculate the dispersion of Pt. Pt particle size was estimated by assuming a spherical particle shape.

The thermogravimetric (TG) analysis of coke formed was carried out using a TGA-50 system (Shimadzu). The oxidation temperature was increased from room temperature to 800 °C at a rate of 10 °C/min under flowing air (25 cm^3/min).

Diffuse reflectance infrared Fourier transformation (DRIFT) spectra of adsorbed CO were recorded by using an IR spectrometer (Bruker, Tensor 27) equipped with a liquid nitrogen cooled MCT detector, a diffuse reflectance accessory (Praying Mantis, Harrick) and a high temperature cell (HVC, Harrick). The cell was fitted with two CaF_2 windows. The catalyst powder of 100 mg was loaded in the sample cup of high temperature cell. The sample was reduced *in situ* at 300 °C (or 500 °C) for 1 h using flowing H_2, and then purged by flowing He for 30 min at the same temperature. After that, the temperature was decreased to 25 °C, and the background spectrum was recorded. 1.11% CO diluted by He was introduced for adsorption for 30 min. The sample was then purged by flowing He for another 30 min. Temperature programmed desorption of CO was performed by increasing the temperature to 450 °C at a rate of 10 °C/min under flowing helium. Spectra were recorded with the background subtracted at a resolution of 4 cm^{-1} and 64 scans accumulation. All spectra were illustrated using Kubelka Munk units, which is linear with the concentration of surface species.

3. Results and discussion

3.1. Chemisorption results

Table 1 gives the results of chemisorption. The dispersion of the PtZr-C sample is 27.9%, and the estimated Pt particle size is 4.1 nm. For the PtZr-PC sample, the dispersion is slightly lower, and the particle size is slightly larger.

3.2. Catalytic performance

Fig. 1 shows the catalytic performance of the two samples for POM at 800 °C during 25 h time on stream. The conversion of CH_4 is declined with time on stream for both samples. A similar trend is observed for H_2 selectivity. In contrast, both CO

Table 1
Chemisorption results of PtZr-C and PtZr-PC

Samples	Dispersion (%)	Average diameter (nm)
PtZr-C	27.9	4.1
PtZr-PC	24.1	4.7

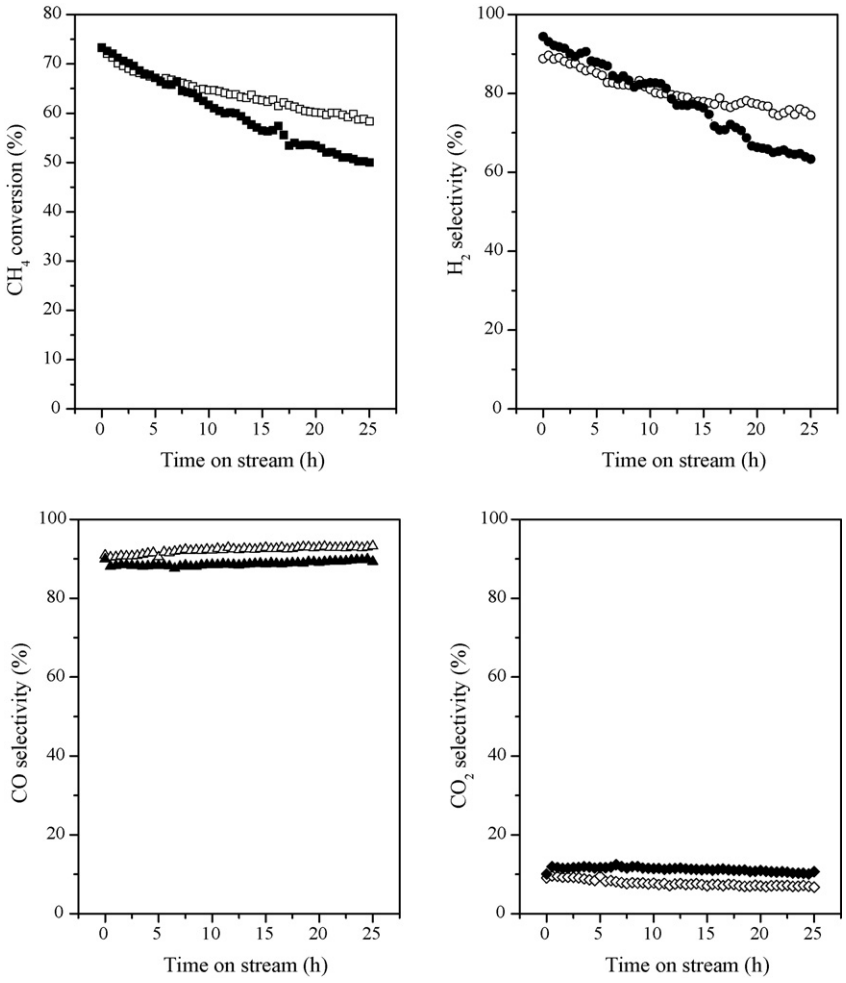

Fig. 1. Stability test of POM over PtZr-C (solid symbols) and PtZr-PC (hollow symbols). Reaction conditions: $T = 800\,^{\circ}C$, $P = 1$ atm, GHSV $= 9 \times 10^4$ cm^3/(g cat h), $CH_4/O_2 = 2{:}1$.

selectivity and CO_2 selectivity only change slightly. A higher CO selectivity with a lower CO_2 selectivity is observed for the PtZr-PC sample. The deactivation rate based on CH_4 conversion is 0.6%/h for the PtZr-PC sample, and it is 0.9%/h for the PtZr-C sample. Obviously, the PtZr-PC sample is more stable during POM reaction.

3.3. Coke analysis

The TG analysis of the samples after 25 h reaction on stream was performed in order to characterize the coke formation. It can be seen from Fig. 2 that the weight loss of both samples is very limited. Considering that the TG analysis was not carried out *in situ* and the sample may adsorb some water and other impurities, little coke was formed on both samples. The TG analyses suggest that the coke formation is not the main reason of catalyst deactivation for the present case. This result is opposite to the case of POM over Pt/Al_2O_3 [17]. A large amount of coke was formed over Pt/Al_2O_3, which leads to deactivation of the catalyst [17]. The good anti-coke performance of Pt/ZrO_2 is probably related to the high mobility of lattice oxygen in ZrO_2 and to the Pt-Zr^{n+} sites that help the elimination of carbon [10].

3.4. IR study of CO adsorption

3.4.1. Effect of reduction temperature

Fig. 3 shows the DRIFT spectra of CO adsorbed on samples (calcined at 600 °C) at 25 °C after the catalysts were reduced at 300 °C for 1 h. The dotted line shows the spectra after CO adsorption for 30 min, and the solid line represents the spectra after CO desorption for 30 min. The gaseous CO band is located at 2173 and 2115 cm^{-1}. The intensity of gaseous CO bands is essentially identical for both PtZr-C and PtZr-PC samples, which make it reasonable to compare both the location and intensity of adsorbed CO bands. All IR bands of adsorbed CO are located at higher wavenumber in the presence of gaseous CO than the bands in the absence of gaseous CO. This is due to the contribution of dipole–dipole interaction between CO molecules at higher CO coverage [25].

For the PtZr-C sample, a band located at 2054 cm^{-1} is observed, accompanied by a shoulder band at 2081 cm^{-1}. A weak and broad band centered at 1813 cm^{-1} is also present, which can be assigned to two or three-fold adsorption of CO [13,14]. The defects sites of Pt particles give a stronger back donation, and thus the metal–carbon bond is strengthened and

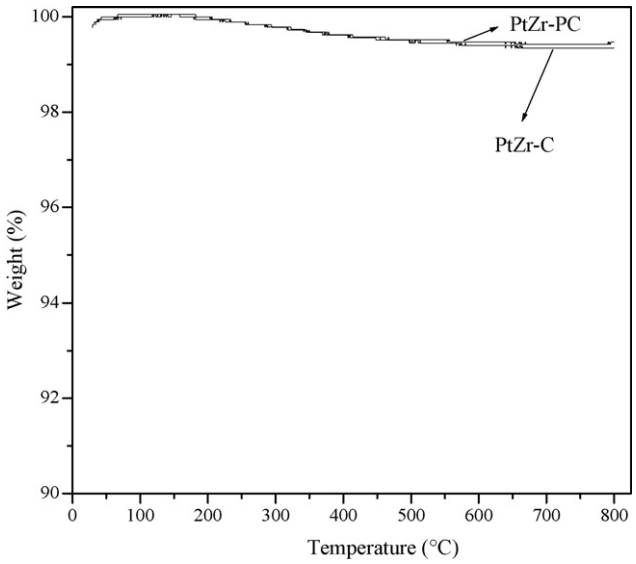

Fig. 2. TGA curves of PtZr-C and PtZr-PC samples after 25 h time on stream at 800 °C of POM.

the carbon–oxygen bond is weakened. Consequently, the carbonyl vibration band of CO adsorbed on defect sites is present at lower wavenumber [26]. We ascribe the band at 2081 cm^{-1} to CO bonded to close-packed planes of Pt particle (such as Pt(1 1 1) plane), and 2054 cm^{-1} to CO bonded to defect sites of Pt particles (such as edges and corners). This is in good accordance with Greenler et al., who assigned three bands at 2081, 2070, and 2063 cm^{-1} to CO linearly adsorbed on planes, edges, and corners of Pt crystallites supported on silica [27].

For the PtZr-PC sample, the band of CO linearly adsorbed on close-packed planes of Pt is also present at 2081 cm^{-1}, whereas the bands of CO linearly adsorbed to defect sites of Pt is blue shifted to 2065 cm^{-1} with respect to that for PtZr-C, and decreased in intensity to appear as a shoulder of the 2081 cm^{-1} band. This suggests that the concentration of defect sites of Pt particles is significantly decreased. In addition, the full width at half maximum (FWHM) of linearly adsorbed CO band for the PtZr-C sample (68 cm^{-1}) is larger than that of the PtZr-PC sample (53 cm^{-1}), indicating that the Pt particle of the PtZr-C sample is smaller than that of the PtZr-PC sample [26].

Fig. 4 gives the DRIFT spectra of CO adsorbed on samples (calcined at 600 °C) at 25 °C after the catalysts were reduced at 500 °C for 1 h. Compared to the spectra reduced at 300 °C, the IR intensity of adsorbed CO decreased sharply for both samples. This decrease in the IR band intensity of adsorbed CO is not a result of the increase in the Pt particle size [28]. It has been suggested that, when the reduction temperature increased to higher than 300 °C, the ZrO_2 near to Pt will be partially reduced to ZrO_x ($x<2$), and migrate onto the surface of Pt particles [28–30]. This state is the so-called strong metal-support interaction (SMSI) [31,32]. As a result, the surface of Pt accessible to CO is decreased. The CO chemisorption capacity is therefore decreased. Thus, 300 °C reduction reflects the true state of

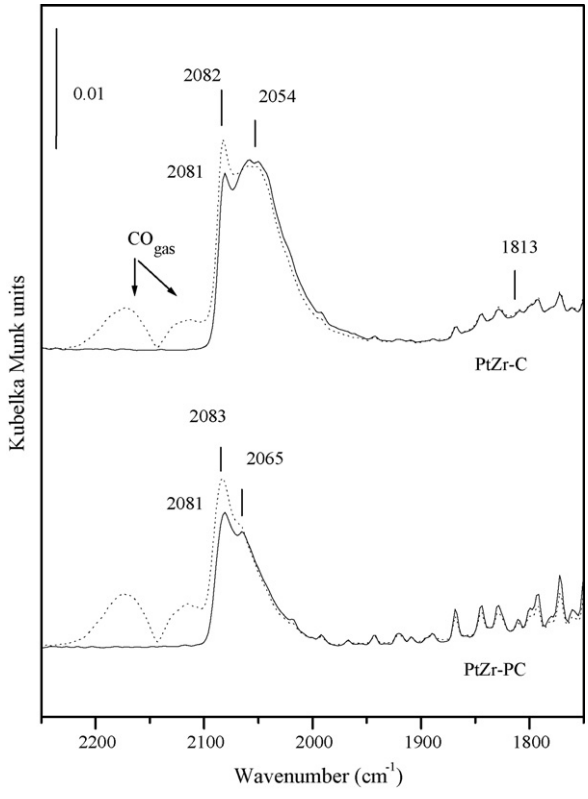

Fig. 3. DRIFT spectra of CO adsorbed on PtZr-C and PtZr-PC catalysts reduced at 300 °C. Dotted line, exposed to 1.11% CO/He for 30 min; solid line, He purged for another 30 min. All spectra were recorded at 25 °C. PtZr-C and PtZr-PC were calcined at 600 °C.

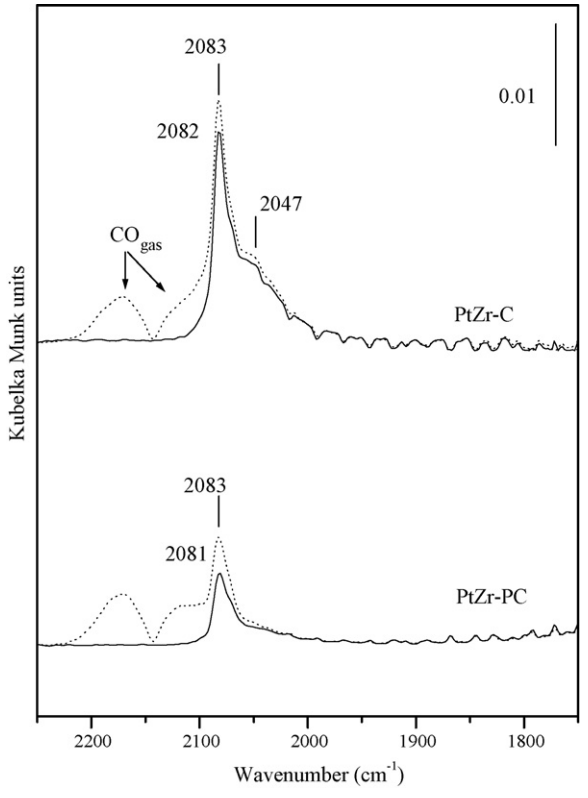

Fig. 4. DRIFT spectra of CO adsorbed on PtZr-C and PtZr-PC catalysts reduced at 500 °C. Dotted line, exposed to 1.11% CO/He for 30 min; solid line, He purged for another 30 min. All spectra were recorded at 25 °C. PtZr-C and PtZr-PC were calcined at 600 °C.

Pt. It should be noted that the peak intensity for the PtZr-C is significantly stronger than that for PtZr-PC, suggesting a lower coverage of ZrO_x on the Pt surface for PtZr-C. The higher coverage of ZrO_x on Pt for PtZr-PC could fix the Pt more strongly on ZrO_2.

3.4.2. Effect of calcination temperature

The catalyst sample was sintered by calcination at different temperatures. Fig. 5 shows the CO adsorption on the catalyst sample calcined at 400 °C for 4 h (Fig. 5A) and 600 °C for 4 h followed by calcination at 800 °C for another 4 h (Fig. 5B). A very intense peak is located at 2070 cm^{-1} along with a shoulder at 2087 cm^{-1}, as well as a very broad band at 1821 cm^{-1}, for the PtZr-C sample. Compared with PtZr-C, a significant decrease in intensity of all adsorbed CO bands is observed for the PtZr-PC sample. Its main band is centered at 2064 cm^{-1} also with a shoulder at 2087 cm^{-1}. These results indicate that, when calcination temperature is 400 °C, the Pt particles in both samples are rough with much higher concentration of defect sites. These results also suggest that the Pt particle of PtZr-C is smaller than that of PtZr-PC when calcination temperature is 400 °C.

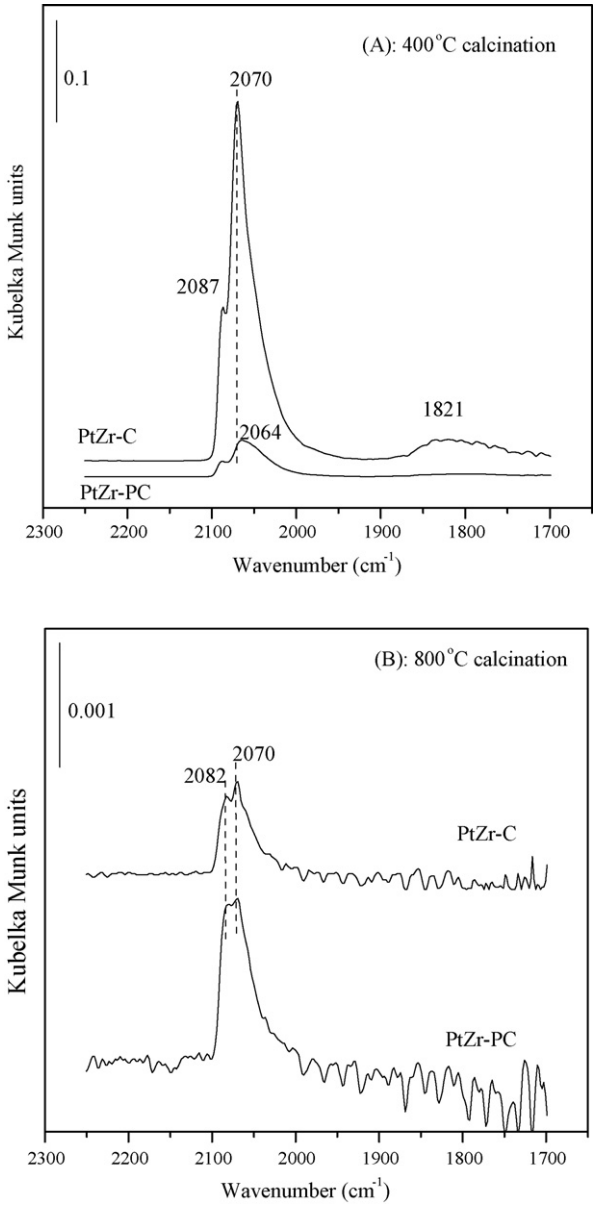

Fig. 5. DRIFT spectra of CO adsorbed on PtZr-C and PtZr-PC catalysts reduced at 300 °C. Procedure: recorded after exposed to 1.11% CO/He for 30 min and He purged for another 30 min. (A) 400 °C calcinations for 4 h; (B) 600 °C calcinations for 4 h followed by 800 °C calcinations for another 4 h. All spectra were recorded at 25 °C.

For the sample calcined at 600 °C for 4 h followed by calcination at 800 °C for another 4 h, all bands reduce significantly, as shown in Fig. 5B. In this case, the IR band of linearly adsorbed CO for the PtZr-PC sample is higher in intensity than that for the PtZr-C sample. This result indicates that the Pt particle size of the PtZr-PC sample is smaller when the sample is further calcined at 800 °C, which has larger surface area for CO coordination.

Fig. 6 shows the change in the IR band intensity of linearly adsorbed CO versus calcination temperature. It can be seen that the IR band intensity decreased sharply with calcination temperature, suggesting that Pt sinters with increasing calcination temperature. The decrease rate is higher for the PtZr-C sample. The results suggest that the plasma treated sample is more resistant to sintering in the presence of O_2 at higher temperatures.

3.4.3. Temperature programmed desorption

Temperature programmed desorption of CO adsorbed on Pt/ZrO_2 catalysts was performed by monitoring IR spectra to obtain the Pt–CO bond strength. Fig. 7 gives the normalized IR intensity of linearly adsorbed CO (CO_L) [33] during the temperature programmed desorption of CO. For both samples, the normalized IR intensity of CO_L passes a maximum at temperature of 100–150 °C, then decreases with increasing temperature. This is due to the fact that the linearly adsorbed CO is more stable than bridge adsorbed CO over Pt catalysts, and a portion of bridge adsorbed CO changes to linearly

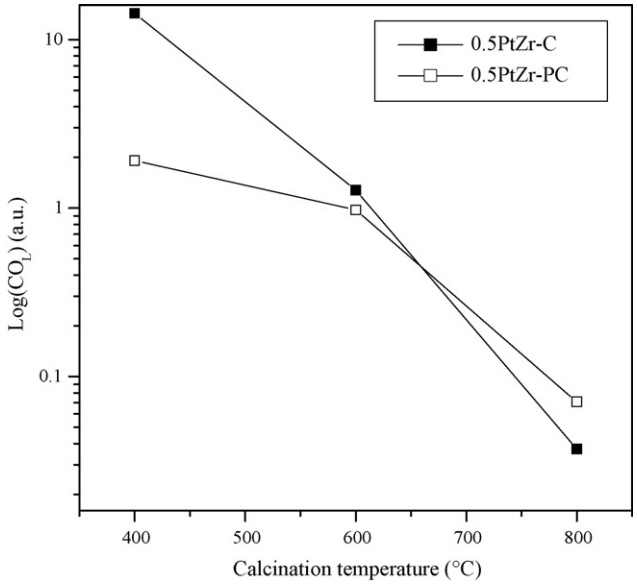

Fig. 6. Changes of integrated IR band intensity of linearly adsorbed CO (CO_L) at 25 °C versus calcination temperature of PtZr-C and PtZr-PC catalysts.

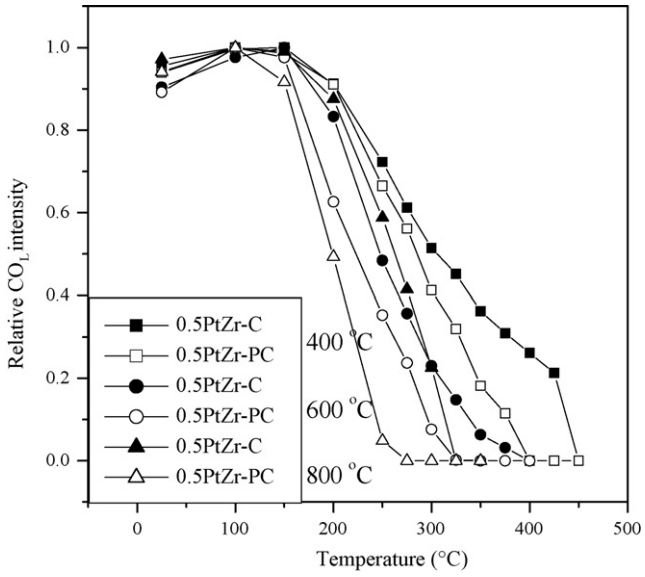

Fig. 7. Changes of normalized relative IR band intensity of linearly adsorbed CO (CO_L) during temperature programmed desorption of CO.

adsorbed CO with increasing temperature [33]. When temperature is further increased, the linearly adsorbed CO begins desorbing.

For both samples, with increasing calcination temperature, the temperature for complete desorption of CO decreases. In general, the defect site concentration decreases (or close-packed plane concentration increases) with increasing particle size, and CO adsorbs linearly on defect sites more strongly than on close-packed planes because of stronger back donation [11–13,26]. Therefore, the CO desorption temperature decreases with increasing calcination temperature, suggesting that the Pt particle size becomes larger.

When the samples are calcined at the same temperature, CO is completely desorbed at lower temperature for the PtZr-PC sample (about 50 °C lower), suggesting that Pt particle of PtZr-PC sample has higher concentration of the close-packed plane, on which CO is expected to be desorbed more easily than on defect sites of the PtZr-C sample [11–13,26]. When the calcination temperatures are 400 and 600 °C, PtZr-PC showed higher concentration of the close-packed plane in line with its larger Pt particle size. When the samples calcined at 600 °C are further calcined at 800 °C, PtZr-PC adsorbs a larger amount of CO (Fig. 5B), but CO is desorbed at lower temperature. Thus, the lower desorption temperature cannot be related to larger Pt particle size but only to higher concentration of the close-packed plane for PtZr-PC, i.e., the smoothened surface of Pt particle.

3.5. Discussion

The TG analysis results show that the coke formed on both samples is very limited. Consequently, the coke formation is not the reason responsible for catalyst deactivation during POM in the present case. Pt sintering in the presence of O_2 is the possible reason accounting for deactivation. There are two pathways to Pt particle sintering: Ostwald ripening (OR) and particle migration and coalescence (PMC) [34]. It was suggested that sintering of the supported Pt particle is limited under the H_2 atmosphere but is much more significant under the oxidizing atmosphere. Datye et al. proposed that Pt sintering is mainly due to the PMC pathway under the H_2 atmosphere [34]. However, the Pt sintering pathway changes to OR in the presence of O_2. It is suggested that the Pt sintering is due to the following reaction:

$$Pt(s) + O_2(g) = PtO_2(g), \quad \Delta H = 175\,kJ/mol$$

The enthalpy of this reaction is much lower than the sublimation energy for Pt (565 kJ/mol) or the energy required for transferring Pt atoms from a particle to the substrate (527 kJ/mol) [34]. Under oxidizing atmosphere, the Pt particle easily becomes volatile PtO_2, which can be readily decomposed into Pt when the temperature is above 600 °C [35]. Thus, PtO_2 helps the migration of Pt atoms from small Pt particles to large Pt particles through the OR pathway. In the present case, the Pt sintering should be easy to occur because of the low specific surface area of ZrO_2 used, on which Pt is difficult to be stabilized.

From the overview point, POM is under reductive atmosphere because H_2 and CO are produced. However, POM over Pt/ZrO_2 follows the reaction pathway of methane combustion followed by CO_2 reforming and steam reforming [9,10]. The reaction of methane combustion is an intensely exothermic reaction under oxidative atmosphere. Methane combustion produces "hot spot" in the catalyst bed [1]; i.e., the actual temperature is higher than 800 °C for the upper layers of the catalyst bed, which is more favorable for Pt sintering through the OR pathway. The Pt atoms could migrate from the upper layers to the lower layers of catalyst bed.

Attempts to observe the sintering of Pt/ZrO_2 catalysts through transmission electron microscopy (TEM) failed because of the low contrast between Pt particles and ZrO_2 and the low amount of Pt loading [28]. However, the intensity of adsorbed CO significantly decreases with increasing calcination temperature (Fig. 6), which strongly supports the Pt sintering under the oxidizing atmosphere.

The IR band intensity of adsorbed CO for the plasma treated sample deceases slowly with increasing calcination temperature compared to that for the untreated sample (Fig. 6). When the sample was calcined at 800 °C for 4 h, the IR intensity of adsorbed CO is higher for the plasma treated sample (Fig. 5B), indicating that the plasma treated sample has a larger surface for CO coordination. Therefore, the plasma treated sample is more resistant to sintering in the presence of O_2 at higher temperatures. The plasma treated sample has higher concentration of the close-packed plane of Pt, which is more difficult to be oxidized than the defect sites. Nagai et al. proposed that Pt sintering could be inhibited through the Pt-support interaction under oxidizing atmosphere [35]. Therefore, the smoothened Pt particles of PtZr-PC probably spread over the ZrO_2 with a larger Pt-ZrO_2 interface, leading to a stronger Pt-support interaction. Moreover, when the samples were reduced at 500 °C, the surface of Pt was more covered by ZrO_x as evidenced by DRIFT spectra of adsorbed CO (Fig. 4) for PtZr-PC, resulting in a tighter Pt fixation during the reaction. The plasma treated sample is more stable than the untreated sample for POM, which is in line with

the finding that the plasma treated sample is more resistant to sintering in the presence of O_2.

4. Conclusion

In this work, plasma treated and untreated Pt/ZrO_2 samples were tested in the reaction of partial oxidation of methane. TG analysis showed little coke formation on both samples, indicating the coke formation is not responsible for the catalyst deactivation. The IR band intensity of adsorbed CO decreases strongly with increasing calcination temperature, suggesting the Pt particle sintering in the presence of O_2. The sintering of plasma treated sample is slower than that of the untreated sample, especially at higher temperature, which indicates that the plasma treated sample is more resistant to sintering under the oxidizing atmosphere. Under the partial oxidation atmosphere, the volatile PtO_2 is easily formed, which helps Pt atom to migrate from small Pt particles to large Pt particles through the Ostwald ripening pathway. The plasma treated sample is more stable for partial oxidation of methane, as a result of its resistance to sintering in the presence of O_2.

Acknowledgments

The supports from National Natural Science Foundation of China (under contract 20490203) and Tianjin Municipal Science and Technology Commission (under contract 043104111) are greatly appreciated. The instrument supports from ABB Switzerland and from the Program for Changjiang Scholars and Innovative Research Team from the Ministry of Education of China are also appreciated.

References

[1] D. Dissanayake, M.P. Rosynek, K.C.C. Kharas, J.H. Lunsford, J. Catal. 132 (1991) 117.
[2] D.H. Hickman, L.D. Schimdt, Science 259 (1993) 343.
[3] S. Alberazzi, P. Arpentinier, F. Basile, P. Del Gallo, G. Fornasari, D. Gary, A. Vaccari, Appl. Catal. A 247 (2003) 1.
[4] J.H. Bitter, K. Seshan, J.A. Lercher, J. Catal. 176 (1998) 93.
[5] A.M. O'Conor, Y. Schuurman, J.R.H. Ross, C. Mirodatos, Catal. Today 115 (2006) 191.
[6] F. Pompeo, N.N. Nichio, M.M.V.M. Souza, D.V. Cesar, O.A. Ferretti, M. Schmal, Appl. Catal. A 316 (2007) 175.
[7] L.V. Mattos, E. Rodino, D.E. Resassco, F.B. Passos, F.B. Noronha, Fuel Process. Technol. 73 (2003) 147.
[8] L.V. Mattos, E.R. Oliveria, P.D. Resende, F.B. Noronha, R.B. Passos, Catal. Today 77 (2002) 245.
[9] F.B. Passos, E.R. Oliveira, L.V. Mattos, F.B. Noronha, Catal. Lett. 110 (2006) 161.
[10] M.M.V.M. Souza, M. Schmal, Catal. Lett. 91 (2003) 11.
[11] G. Blyholder, J. Phys. Chem. 68 (1964) 2772.
[12] S.G. Podkolzin, J.Y. Shen, J.J. de Pablo, J.A. Dumesic, J. Phys. Chem. B 104 (2000) 4169.
[13] T. Visser, T.A. Nijhuis, A.M.J. van der Eerden, K. Jenken, Y. Ji, W. Bras, S. Nikitenko, Y. Ikeda, M. Lepage, B.M. Weckhuysen, J. Phys. Chem. B 109 (2005) 3822.
[14] J.A. Anderson, F.K. Chong, C.H. Rochester, J. Mol. Catal. A 140 (1999) 65.
[15] J. Llorca, N. Homs, J. Araña, J. Sales, P.R. de la Piscina, Appl. Surf. Sci. 134 (1998) 217.
[16] Y.H. Hu, E. Ruckenstein, Adv. Catal. 48 (2004) 297.
[17] X.L. Zhu, P.P. Huo, Y.P. Zhang, C.J. Liu, Ind. Eng. Chem. Res. 45 (2006) 8604.
[18] J.G. Wang, C.J. Liu, Y.P. Zhang, K.L. Yu, X.L. Zhu, F. He, Catal. Today 89 (2004) 183.
[19] C.J. Liu, G.P. Vissokov, B.W.L. Jang, Catal. Today 72 (2002) 173.
[20] J.-J. Zou, C.J. Liu, Y.P. Zhang, Langmuir 22 (2006) 2334.
[21] C.K. Shi, B.W.L. Jang, Ind. Eng. Chem. Res. 45 (2006) 5879.
[22] Z.H. Li, S.X. Tian, H.T. Wang, H.B. Tian, J. Mol. Catal. A 211 (2004) 149.
[23] Z.-J. Wang, Y. Zhao, L. Cui, H. Du, P. Yao, C.-J. Liu, Green Chem. 9 (2007) 554.
[24] X.L. Zhu, K.L. Yu, J. Li, Y.P. Zhang, Q. Xia, C.J. Liu, React. Kinet. Catal. Lett. 87 (2005) 93.
[25] P. Bazin, O. Saur, J.C. Lavalley, M. Daturi, G. Blanchard, Phys. Chem. Chem. Phys. 7 (2005) 187.
[26] H. Song, R.M. Rioux, J.D. Hoefelmeyer, R. Komor, K. Niesz, M. Grass, P. Yang, G.A. Somorjai, J. Am. Chem. Soc. 128 (2006) 3027.
[27] R.G. Greenler, K.D. Burch, K. Kretzschar, R. Klauser, A.M. Bradshaw, Surf. Sci. 152–153 (1985) 336.
[28] J.H. Bitter, K. Seshan, J.A. Lercher, Top. Catal. 10 (2000) 295.
[29] D. Tibiletti, F.C. Meutier, A. Goguet, D. Reid, R. Burch, M. Boaro, M. Vicario, A. Trovarelli, J. Catal. 244 (2006) 183.
[30] S. Ricote, G. Jacobs, M. Milling, Y. Ji, P.M. Patterson, B.H. Davis, Appl. Catal. A 303 (2006) 35.
[31] S.J. Tauster, S.C. Fung, R.L. Garten, J. Am. Chem. Soc. 100 (1978) 170.
[32] S. Bernal, J.J. Calvino, M.A. Cauqui, J.M. Gatica, C. Larese, J.A. Pérez Omil, J.M. Pintadom, Catal. Today 50 (1999) 175.
[33] S. Zafeiratos, G. Papakonstantinou, M.M. Jacksic, S.G. Neophytides, J. Catal. 232 (2005) 127.
[34] A.K. Datye, Q. Xu, K.C. Kharas, J.M. McCarty, Catal. Today 111 (2006) 59.
[35] Y. Nagai, T. Hirabayashi, K. Dohmae, N. Takagi, T. Minami, H. Shinjoh, S. Matsumoto, J. Catal. 242 (2006) 103.